Journal of Visualization, Vol. 11, No. 4 (2008)365-373

Regular Paper

Visualization of Aerodynamic Noise Source around a Rotating Fan Blade

Nashimoto, A.*[1], Fujisawa, N.*[2], Nakano, T.*[1] and Yoda, T.*[3]

*1 Mitsuba Corporation, 598, No, Niisato, Kiryu, Gunma, 376-0122, Japan. E-mail: a-nashi@mitsuba.co.jp
*2 Visualization Research Center, Niigata University, 8050 Ikarashi 2, Niigata, 950-2181, Japan.
*3 Mitsuba Corporation, 1-2681, Hirosawa, Kiryu, Gunma, 376-8555, Japan.

Received 28 December 2007
Revised 25 June 2008

Abstract : The purpose of this study is to understand the aerodynamic noise source distribution around a rotating fan blade by measuring the noise signal and velocity field around the blade. The local noise-level distribution over the fan blade is measured by microphone arrays, and the flow field is visualized by smoke and phase-averaged PIV measurement. The noise source distribution is examined by cross-correlation analysis between noise signal and velocity fluctuation. It is found that the noise source is located near the rotating fan blade, especially around leading and trailing edges. The separation and reattachment of flow are observed near the leading edge, and the tip vortices and vortex shedding are found near the trailing edge. The cross-correlation distribution of the noise signal and the radial velocity fluctuation shows large magnitude in the correlated regions, which indicates the noise generation by the formation of vortex structure around the blade.

Keywords : Aerodynamic noise, Noise source, Flow visualization, PIV, Fan, Measurement.

1. Introduction

Aerodynamic noise is often observed in rotating machinery, such as fan (Sharland, 1964), helicopter rotor (George et al., 1984), and wind turbine blade (Hubbard et al., 1991). The detection of such noise source and its control have been topics of interests for many years. Based on the results of previous studies, the noise source of a rotating-machinery is categorized into the mechanical noise caused by mechanical contact and the aerodynamic noise due to the aerodynamic interference between the blade and the flow field, which is known as separation, reattachment and vortex shedding. The aerodynamic noise has been considered more important than the mechanical noise, when the flow velocity increases. From flow visualization experiments, it was found that the aerodynamic noise of such machinery is generated by the vortex shedding from the trailing edge (Kotake, 1975; Howe, 1978; Arbey et al., 1983; Manoha et al., 2000) and by the tip vortex (Brooks et al., 1986). However, the noise source location and the generation mechanism depend on blade and casing conditions for the prototype fan. For this reason, experimental technique for detecting noise source location is a key issue in the present state of the aerodynamic noise study (Iida et al., 2007).

Generally speaking, the detection of the noise source can be conducted by experimental techniques, such as sound intensity (Gloza, 2002), acoustic holography (Brutel-Vuilmet, C. et al., 2006), and the distance measurement between the sound source and sensors (Fujisawa et al., 2001).

However, these techniques have been rarely applied to rotating machinery because of its unsteady nature of the flow field and the complexity of the noise source distribution. To address this issue, a local noise level measurement is carried out on a rotating fan using a microphone arrays (Nashimoto et al., 2006). As a result, the noise source distribution around the leading and the trailing edge of the fan blade was visualized and the effectiveness of the measurement was confirmed. With this method, however, it is impossible to identify the flow structure regarding the noise generation with high spatial resolution. On the other hand, as for the flow field around the fan blade, the flow field is visualized by oil film and smoke (Nashimoto et al., 2000), and the velocity field is measured by laser doppler velocimetry (Nash, 1999; Cai et al., 2002) and particle image velocimetry (Nashimoto et al., 2004). Although these studies on flow field around the fan blade allow for the understanding of flow phenomena, such as separation, reattachment and vortex shedding, these techniques are not suitable for identifying the noise source distribution. For such a problem, cross-correlation analysis of noise signal and velocity fluctuation provides an effective measure for visualizing the noise source distribution (Nakano et al., 2006), which is originally developed for the detection of discrete frequency noise source from a symmetrical airfoil (Takagi et al., 2006; Nakano et al., 2007; Oguma et al., 2007). In this technique, flow structure regarding noise generation is detected by cross-correlation analysis, and the generation mechanism of aerodynamic noise is examined through the flow structure related to the noise generation. This technique is considered to be effective on a rotating fan as well.

In the present study, we employ noise source detection by local noise level measurement, the flow visualization, the phase-averaged PIV measurement, and cross-correlation analysis by simultaneous measurement of noise signal and velocity fluctuation. Then, the mechanism of aerodynamic noise from a rotating fan is visualized based on these experimental results.

2. Experimental Apparatus and Procedures

2.1 Experimental Apparatus

Figure 1(a) shows a schematic view of the experimental setup. The test fan is a cooling fan for automobile, having a diameter of 280 mm with four blades, which is shown in Fig. 1(b). The fan rotates at 2000 ± 2 rpm in the present experiment conducted in a semi-anechoic chamber having a background noise level of 24 dB. The microphone is a 1/2 inch-long capacitive one, which covers the frequency range from 20 Hz to 20 kHz. The output signal from microphone amplifier is digitally converted into the noise signal in the computer. The coordinate system X, Y, Z used in the present study is shown in Fig. 1(a), where Z is the axial distance from the boss of the fan blade.

Figure 1(c) shows the measuring areas near the leading and trailing edges, both of which are in y-z plane. In each area, both noise measurement with a microphone and phase-averaged PIV measurement of flow field are conducted. Target area 1 is located near the leading edge. The center of this area represents the radial position120 mm from the rotor center, which shows the peak noise-source position measured by the microphone. The area of measurement ($= 28 \times 28$ mm^2) is large enough to study the flow phenomena, such as separation and reattachment on leading edge. Microphone #1 is set at a distance 25 mm from leading edge of the suction surface to prevent being caught in images. Target 2 is located near the trailing edge. The center of the target area 2 corresponds to 138 mm from the rotor center. The target area 2 is 34×34 mm^2, which is large enough to observe the tip vortices and the vortex shedding from the trailing edge. Microphone #2 is set at a distance 20 mm outside of blade edge in radial direction to prevent being caught by images. For both targets, the centers of image and microphone are aligned.

2.2 Flow Visualization and PIV Measurement

The flow visualization around a rotating fan was carried out using smoke from a smoke generator. The size of the smoke particle is about 1 μm in diameter. The flow field is illuminated by a laser light sheet from double pulsed Nd:YAG lasers (30 mJ/pulse) and the images are taken by a monochrome

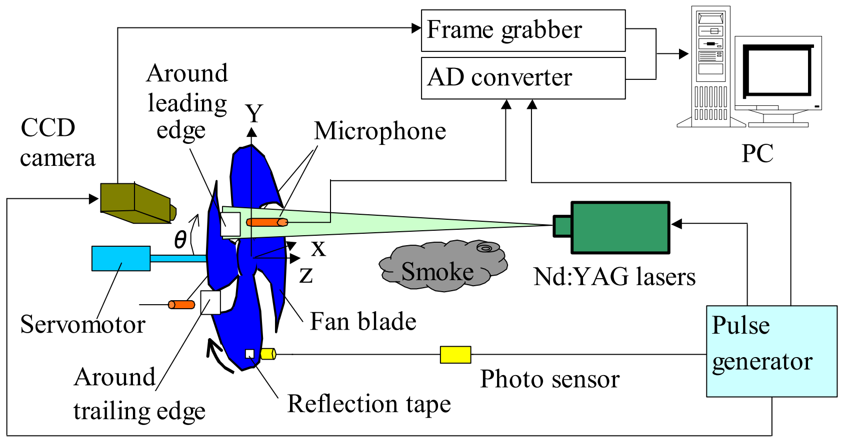

(a) Experimental setup

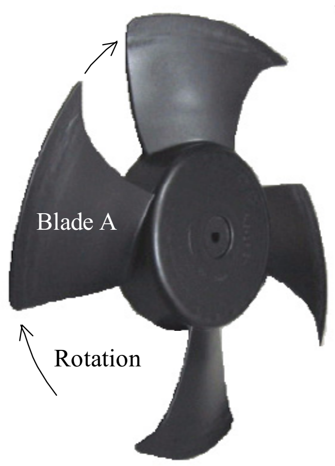

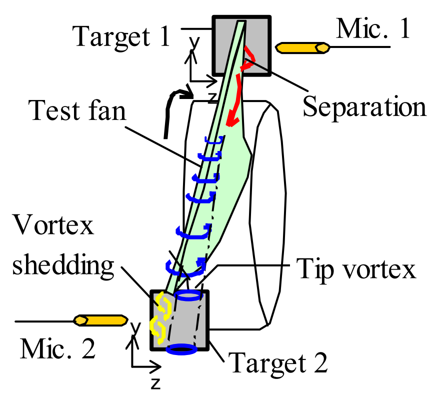

(b) Test fan (c) Close-up view of blade A

Fig. 1. Experimental arrangement for simultaneous measurement of noise and velocity fluctuation.

CCD camera with frame straddling function. The camera outputs images with 8 bits in gray level having a spatial resolution of 1017×1008 pixels. The illumination of lasers is synchronized with the camera through the signal from the pulse generator. The captured image shows that the diameter of tracer particle is about 2 pixels. The images used for the phase-averaged PIV measurement are obtained with reference to the blade position signals from the photo sensor. In the PIV analysis, the direct cross-correlation algorithm in combination with sub-pixel analysis is employed using the commercial software VidPIV. A square correlation window is used in the PIV analysis with the size of 32 × 32 pixels, which is overlapped with the neighboring windows by 50 %. The erroneous velocity vectors in the flow field were less than 1 % of the total number of analyzed velocity vectors, and they were removed from the results. It should be mentioned that the PIV analysis nearest to the blade is not considered in the present results, because they are unreliable in accuracy due to the smaller number of tracer particles in the correlation windows near the surface. In the present experiment, the time interval between two sequential images is set to 5 μs, so that the maximum particle displacement is about 4 pixels. Based on the result of the uncertainty analysis, the uncertainty interval in the PIV measurement is estimated as 3 % with confidence level of 95 %.

2.3 Simultaneous Measurement of Noise and Velocity Fluctuation

Simultaneous measurement of noise and velocity fluctuation is carried out to understand the relationship between the noise and the flow field at the fixed blade-position of the fan. The signals from photo sensor and microphone are simultaneously sampled using an AD converter. In order to correlate the noise signal and the velocity fluctuation from PIV images, the corresponding noise data was selected from the time-series noise signal by considering the delay time of the sound transmitting from fan surface to microphone. Therefore, the phase-averaged measurement was conducted to obtain the cross-correlation distribution. The concept of cross-correlation here is the correlation between the noise signal at the microphone and velocity fluctuation in the target area, which allows the extraction of noise source distribution in the target area. In this experiment, 5,000 sets of PIV images and noise signals are analyzed in order to gain phase-averaged results. The experimental time required for obtaining these data is about 1,000 seconds. Using these experimental data, the cross correlation between the noise signal and the velocity fluctuation is evaluated. The correlation coefficient between the noise signal and normal velocity fluctuation R_{vp} is defined by $R_{vp} = \overline{v'p'}/(V_r \times p_{rms})$, and the correlation coefficient between noise signal and axial velocity fluctuation R_{wp} is defined by $R_{wp} = \overline{w'p'}/(V_r \times p_{rms})$. Note that these measurements were made dimensionless by circumferential velocity V_r, and v' and w' are the radial and axial velocity fluctuations, respectively, and p' is noise fluctuation, p_{rms} is rms sound pressure level.

3. Results and Discussions

3.1 Noise Characteristics

Figure 2 shows contour maps of local noise level obtained from microphone-array measurement. The local noise data is sampled with reference to the photo sensor and are phase-averaged. The detailed experimental method for the measurement has been explained by Nashimoto et al. (2006). The results are on the suction surface in x-y plane (a) and from the side in x-z plane (b), which are taken at rotating speed of the fan at 2000 rms. The Reynolds number based on the fan diameter is $Re = 2.7 \times 10^5$. The grid intersections in these figures represent the location of microphones in the measurement. The result in x-y plane (a) indicates that the noise sources are mainly distributed around the leading and the trailing edges of the blade, and the noise level is found to be highest near the leading edge. Figure 2(b) in x-z plane indicates that the noise sources are mainly distributed on the suction sides of the blade near the leading and trailing edges. Note that the angle θ represents the circumferential angle of the blade.

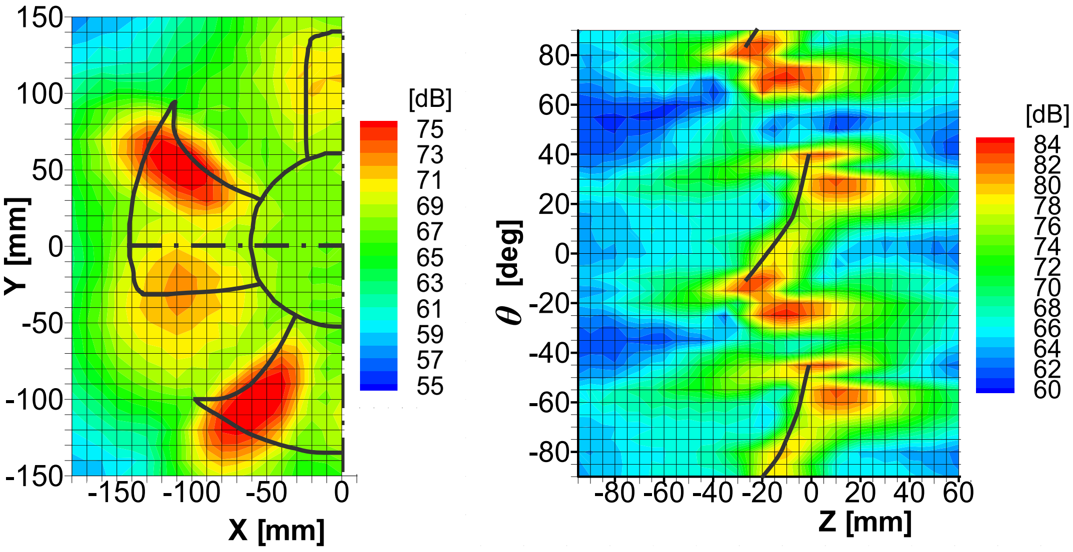

(a) Suction side (b) Side view

Fig. 2. Distributions of sound pressure level on rotating blade.

3.2 Flow Visualization

Figures 3(a) and (b) show the instantaneous flow visualizations around the leading (Target 1 in Fig.1(c)) and trailing edges (Target 2 in Fig.1(c)) of the fan blade, respectively, which are observed from the side of the fan. The visualized smoke image around leading edge is shown in Fig. 3(a). It can be seen that the flow separation occurs near the leading edge of the blade and the following flow reattachment is observed in the downstream. Thus, the small separation bubble is formed just downstream of the leading edge of the suction side of the blade. In this image, the black colored and elongated shape on the left is a part of blade and the black area on the left is the shadow of the blade. On the other hand, the flow visualization around the trailing edge of the blade is shown in Fig. 3(b). The white shining part on upper left in Fig. 3(b) is the trailing edge of the blade and the black area on its left is the shadow of the trailing edge. It should be mentioned that the black area at the center is a part of the vortex core originated from the blade tip, and the vortices shed from the trailing edge are seen on the left side of the tip vortices. There are rather small numbers of smoke particles in the core region of the vortices, which is due to the presence of centrifugal forces on the smoke particles. Note that the tip vortices are generated from the upstream blade due to the roll-up flow from the pressure side to the suction side of the blade. For details, see the flow visualization study by Nashimoto et al. (2004). The trailing edge vortices are Karman vortices shed alternatively from pressure and suction surfaces of the trailing edge of the blade. Therefore, the interference between the tip vortices and the trailing edge vortices is observed in the downstream side. The width of trailing edge vortices is much smaller than that of the wake of tip vortices. From these results of flow visualization, complicated flows, such as separation near leading edge and vortex formation near trailing edge, are observed, and their locations almost correspond to the areas of high-level local noise in Fig. 2. Therefore, these phenomena are considered to be the causes of aerodynamic noise generation from the fan blade.

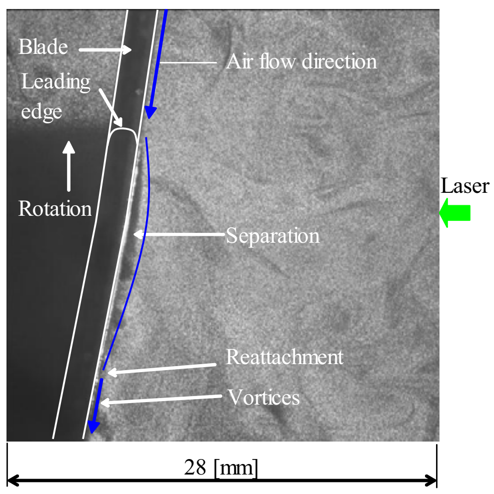

(a) Target 1 (Around leading edge)

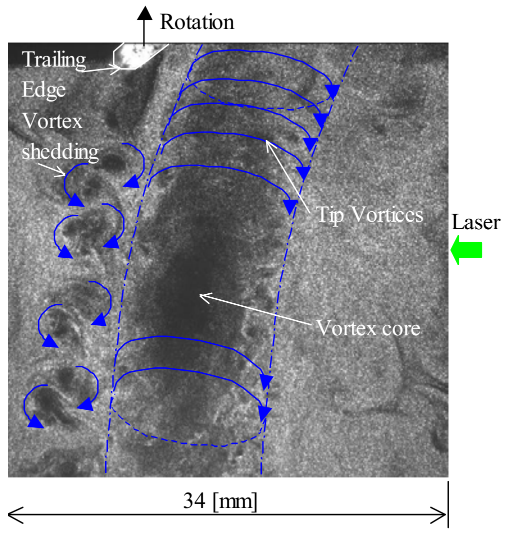

(b) Target 2 (Around trailing edge)

Fig. 3. Flow field visualization of noise sources.

3.3 PIV Measurement of Velocity Field

Figure 4 shows the phase-averaged flow properties, such as relative mean velocity $V_{dl} = (V - V_r)/V_r$, radial velocity fluctuation, and axial velocity fluctuation, respectively, around the leading edge of the fan blade. These distributions are made dimensionless by circumferential velocity V_r. According to Fig. 4(a), the flow over the blade surface is accelerated on the suction side near the leading edge, but it separates immediately downstream of the accelerated region. In this separated region, the velocity fluctuations grow slightly, as shown in Figs. 4(b) and (c). Therefore, the separated boundary layer over the blade surface is expected to be in a turbulent state due to the presence of turbulence in the flow. Although the reattachment of the separated boundary layer is not clearly observed in Fig. 4, the boundary layer tends to reattach on the surface downstream, as shown in Fig. 3(a). It should be mentioned that the velocity fluctuations are lower in the upstream of the separation region due to the presence of the highly accelerated region over the fan blade, while the

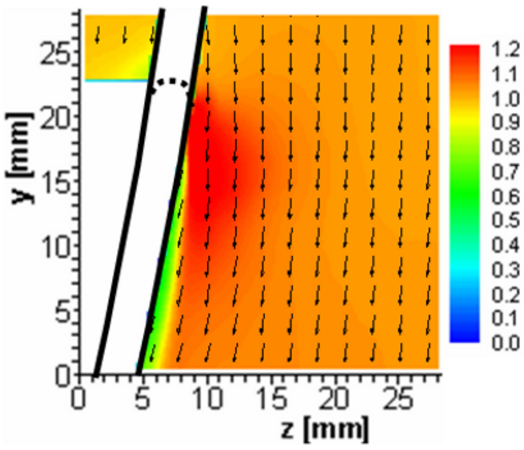

(a) Relative velocity field

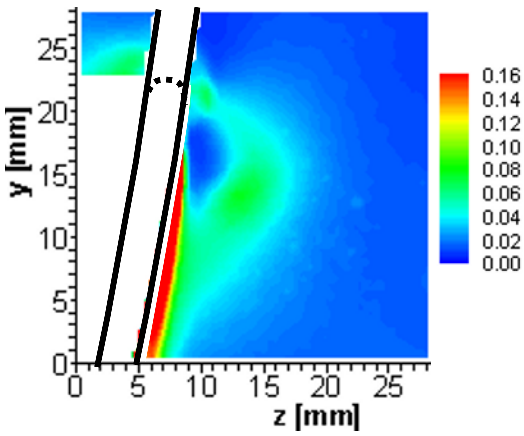

(b) Radial velocity fluctuation

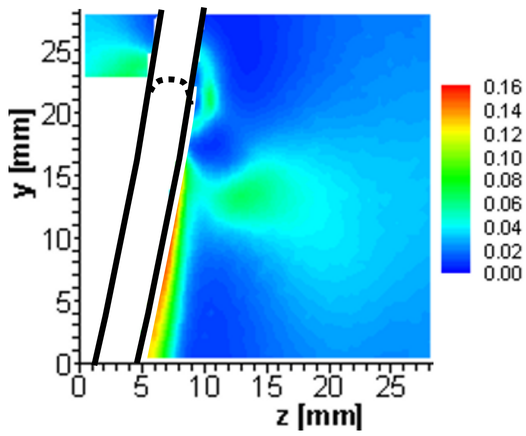

(c) Axial velocity fluctuation

Fig. 4. Phase-averaged flow properties around the leading edge of a blade.

velocity fluctuations increase slightly in the decelerated region away from the blade.

Figure 5 shows the corresponding flow properties around the trailing edge. Lower velocity area is formed near the trailing edge due to the presence of the near-wake velocity profile. While, the higher velocity area is observed over the suction surface of the blade, which is caused by the formation of the tip vortices, as was observed in Fig. 3(b). On the other hand, the velocity fluctuation increases near the trailing edge and over the suction surface of the blade, which suggests the presence of noise sources in these areas.

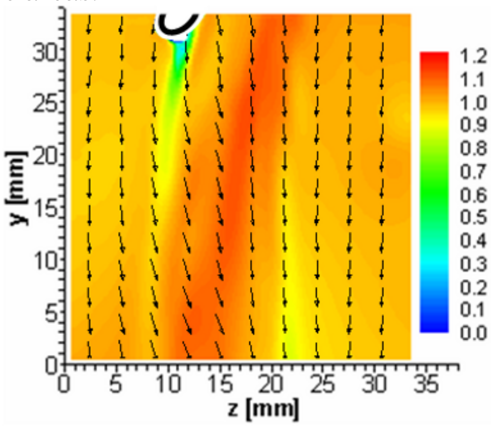

(a) Relative velocity field

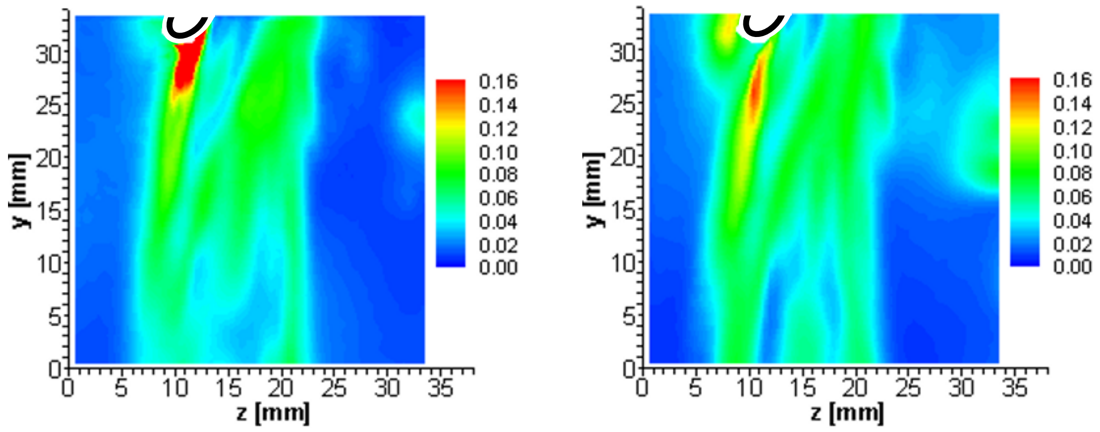

(b) Radial velocity fluctuation (c) Axial velocity fluctuation

Fig. 5. Phase-averaged flow properties around the trailing edge of a blade.

3.4 Cross-Correlation between Noise and Flow

Figure 6 shows the cross-correlation contours of noise signal and velocity fluctuation around the leading edge of the blade. The correlation with the radial velocity fluctuation is shown in Fig. 6(a) and that with the axial velocity fluctuation is in Fig. 6(b). It is found from Fig. 6(a) that the positive correlation exists in the separation region near the blade and the negative correlation is located over the leading edge of the blade. For the radial velocity fluctuation (Fig. 6(a)), the correlation values are mostly negative except for the near-wall region. For the axial velocity fluctuation (Fig. 6(b)), however, the correlation is changed to positive values in most of the area. Such difference in the correlation sign may be due to the structure of turbulence associated with the noise generation. It can be considered from these results that the separation area and the outside area are the noise source locations of the fan. Also, these areas having high correlation correspond to the region with large velocity fluctuation, as shown in Figs. 4(a) and (b). Therefore, the present results indicate that the region of noise source is closely related to the area of large velocity fluctuations.

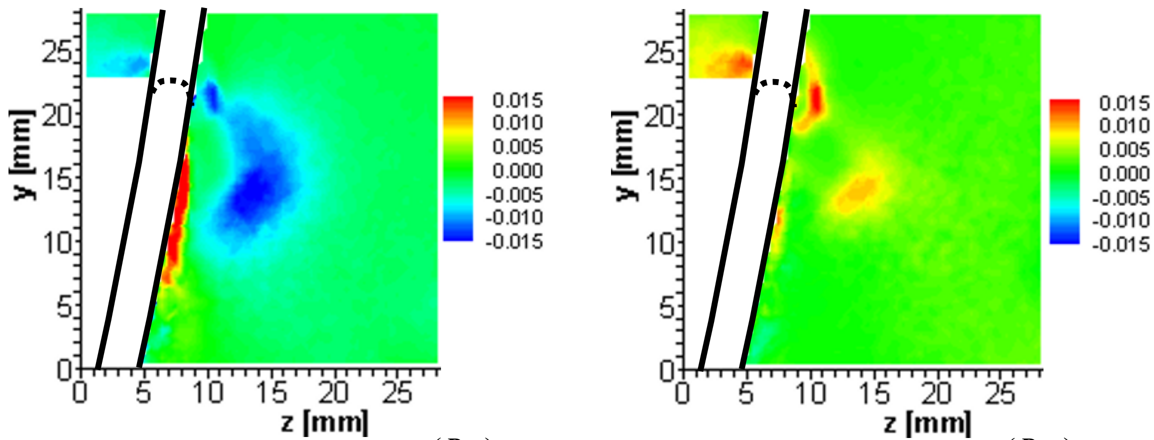

(a) Radial velocity fluctuation (R_{vp}) (b) Axial velocity fluctuation (R_{wp})

Fig. 6. Correlation of noise signal and velocity fluctuation around leading edge.

Figure 7 shows the cross-correlation contours of noise and velocity fluctuation around the trailing edge of the blade. The correlation with radial velocity fluctuation is shown in Fig. 7(a), and that with axial velocity fluctuation is shown in Fig. 7(b). These results show that high correlation areas are recognized over a wide range along the tip vortices and in the areas of vortex shedding from the trailing edge. These high correlation areas are expected to correspond to the noise source region of a rotating fan. The highly correlated area of noise signal with the axial velocity fluctuation is similarly observed in that with the radial velocity fluctuation, so that they are closely related with each other. However, the sign of correlation for the radial velocity fluctuation is both positive and negative, and that for the axial velocity fluctuation is shifted to a positive side, which shows the presence of the highly turbulent vortex structure around the trailing edge. This result indicates that the tip vortices and the vortex shedding generated from the trailing edge of the blade are important noise sources of a rotating fan. Compared to the noise source obtained from the local noise level measurement by microphone arrays, these results show the detailed structure of noise source distribution. Thus, the present method allows for the detection of the noise source locations with higher spatial resolution than the local noise level measurement.

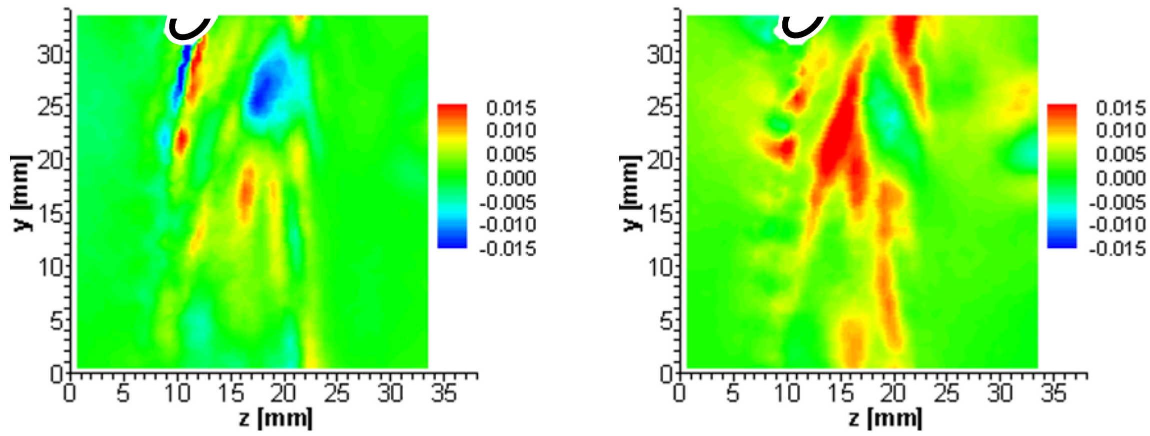

(a) Radial velocity fluctuation (R_{vp}) (b) Axial velocity fluctuation (R_{wp})

Fig. 7. Correlation of noise signal and velocity fluctuation around trailing edge.

4. Conclusion

In order to clarify the noise sources and their flow structure of rotating fan blade for automobiles, an experimental study was carried out by means of microphone array, smoke visualization, PIV measurement, and cross-correlation measurement of noise signal and velocity fluctuation. As a result of local noise level measurement by microphone arrays, the maximum noise level was found around leading and trailing edge of the blade. The flow visualization by smoke and the phase-averaged PIV measurement show that the separation and reattachment of the flow over the suction surface of the blade are observed around the leading edge, and tip vortices and vortex shedding are found around the trailing edge. Based on the evaluation of cross-correlation between noise signal and velocity fluctuation, the noise source contours are found at the corresponding areas with high spatial resolution, which indicates the usefulness of the noise source measurement. The cross-correlation between the noise signal and the radial velocity fluctuation shows an alternating sign, corresponding to the vortex structure associated with the noise source distribution.

References

Arbey, H. and Bataille, J., Noise Generated by Airfoil Profiles Placed in a Uniform Laminar Flow, The Journal of Fluid Mechanics, 134 (1983), 33-47.

Brooks, T. F. and Marcolini, M. A., Airfoil Tip Vortex Formation Noise, AIAA Journal, 24-2 (1986), 246-252.

Brutel-Vuilmet, C., Guigou-Carter, C., Villot, M. and Jean, P., Measurement of the Sound Reduction Index as a Function of the Incidence Angle by Two Different Methods, Building Acoustics, 13-1 (2006), 33-48.

Cai, W. X., Shiomi, N., Sasaki, K., Kaneko, K. and Setoguchi, T., Visualization of Tip Vortex Flow in an Open Axial Fan by EFD, Journal of Visualization, 5-3 (2002), 293-300.

Fujisawa, N., Shibuya, S., Nashimoto, A. and Takano, T., Aerodynamic Noise and Flow Visualization around Two-dimensional Airfoil, Journal of the Visualization Society of Japan, 21-9 (2001), 123-129 (in Japanese).

George, A. R. and Chou, S. T., Comparison of Broadband Noise Mechanisms, Analyses and Experiments on Rotors, Journal of Aircraft, 21-8 (1984), 583-592.

Gloza, I., Tracking the Underwater Noise Source Using a Vector Sound-intensity Probe, Acta Acustica united with Acustica, 88-5 (2002), 670-673.

Howe, M. S., A Review of the Theory of Trailing Edge Noise, Journal of Sound and Vibration, 61-3 (1978), 437-465.

Hubbard, H. H. and Shepherd, K. P., Aeroacoustics of Large Wind Turbines, Journal of the Acoustical Society of America, 89-6 (1991), 2495-2508.

Iida, A., Mizuno, A. and Kato, C., Identification of Aerodynamic Sound Source with a Compact Green's Function, Journal of

Visualization, 10-2 (2007), 161-162.
Kotake, S., Random Vortex Shedding Noise of Airfoils, Journal of Sound and Vibration, 40-1 (1975), 87-99.
Manoha, E., Troff, B. and Sagaut, P., Trailing-Edge Noise Prediction Using Large-Eddy Simulation and Acoustic Analogy, AIAA Journal, 38-4 (2000), 575-583.
Nakano, T., Fujisawa, N. and Lee, S., Measurement of Tonal-Noise Characteristics and Periodic Flow Structure around NACA0018 Airfoil, Experiments in Fluids, 40-3 (2006), 482-490.
Nakano, T., Fujisawa, N., Oguma, Y., Takagi, Y. and Lee, S., Experimental Study on Flow and Noise Characteristics of NACA0018 Airfoil, Journal of Wind Engineering and Industrial Aerodynamics, 95 (2007), 511-531.
Nash, E. C., Lowson, M. V. and McAlpine, A., Boundary Layer Instability Noise on Airfoils, The Journal of Fluid Mechanics, 382 (1999), 27-61.
Nashimoto, A., Fujisawa, N., Akuto, T. and Nagase ,Y., Measurement of Aerodynamic Noise and Wake Flow Field in a Cooling Fan with Winglets, Journal of Visualization, 7-1 (2004), 85-92.
Nashimoto, A., Fujisawa, N., Kimura, E. and Akuto, T., Visualization of Surface Flow over a Blade of Rotating Machinery by Oil-Film Technique and Measurement of Shear Stress Distribution by Image Analysis, Journal of the Visualization Society of Japan, 20-79 (2000), 56-61(in Japanese).
Nashimoto, A., Fujisawa, N., and Sasaki, H., Visualization of Noise Sources and Surface Flows over a Rotating Fan Blade, Journal of Visualization, 9-3 (2006), 245-246.
Oguma, Y. and Fujisawa, N., Near-wall Velocity Measurement over an Airfoil by PIV, Journal of Visualization, 10-2 (2007), 157-158.
Sharland, I. J., Source of Noise in Axial Flow Fans, Journal of Sound and Vibration, 1-3 (1964), 302-322.
Takagi, Y., Fujisawa, N. and Nakano, T., Cylinder Wake Influence on the Tonal Noise and Aerodynamic Characteristics of a NACA0018, Journal of Sound and Vibration, 297 (2006), 563-577.

Author Profile

Atsushi Nashimoto: He graduated from Graduate School of Niigata University and received a degree of Dr. Eng. in 2007. He has been working at Mitsuba Corporation since 1972, and now he is a senior researcher in the Technical Development Department. His current research interests are flow visualization and measurement of noise from rotating machinery.

Nobuyuki Fujisawa: After graduating from Graduate School of Tohoku University (D.E. 1983), he joined Gunma University in 1983 and worked as an associate professor in 1991. Since 1997, he has been a professor of Niigata University and is currently a director of Visualization Research Center at Niigata University. His current research interests are visualization and non-intrusive measurement of velocity and temperature field of complex flow and the flow accelerated corrosion and erosion problems of highly aged nuclear power plant.

Takeshi Yoda: After graduating from Nihon University in 1979, he joined Mitsuba Corporation in 1981. From 1981 to 1990, he engaged on development of motorcycle generator in the Design Section, from 1990 to 1997, CAE/noise vibration analysis in the Research Department, and since 1998, he has been working on CAE analysis in the Technical Development Department. Now he is the Department Manager.

Tomonori Nakano: After graduating from Graduate School of Niigata University (D.E. 2006), he joined Mitsuba Corporation in 2006 and since then, has been working on various kinds of flow visualization experiments in the Technical Development Department.